IOP Conf. Series: Materials Science and Engineering **192** (2017) 012030 doi:10.1088/1757-899X/192/1/012030

Influence of tiny amounts of impurity on dendritic growth in undercooled melts

O V Kazak[1] **P K Galenko**[1,2] **D V Alexandrov**[1]

[1] Ural Federal University, Laboratory of Multi-Scale Mathematical Modeling, Department of Theoretical and Mathematical Physics, 620000 Ekaterinburg, Russian Federation
[2] Friedrich-Schiller-Universität Jena, Physikalisch-Astronomische Fakultät, D-07743 Jena, Germany

E-mail: olegkazak@yandex.ru · peter.galenko@uni-jena.de · dmitri.alexandrov@urfu.ru

Abstract. An influence of small amounts of impurity on the dendrite growth is investigated analytically and numerically. For investigations, a model for anisotropic dendrites rapidly growing in pure and binary melts is used. The dependence of the dendrite growth velocity and of the dendrite tip radius from undercooled melt from amounts of impurity is analyzed. Calculations are carried out for the pure nickel and binary nickel-zircon diluted melts.

1. Introduction

Crystallisation process is one of the most important phase transformations in industrial production. It plays a crucial role in casting and foundry industry. The present work is devoted to the kinetics of dendritic growth from an undercooled pure nickel melt in comparison with the dendrite growth kinetics in highly diluted and diluted nickel-zircon melts.

Solidification of undercooled Ni-Zr alloys has been investigated in [1,2] at small concentrations of Zr using dendritic growth velocities V measured in Ref. [1] as a function of undercooling ΔT in levitated droplets of $Ni_{99}Zr_1$ alloys using electromagnetic levitation technique [3]. These results have been described within the LKT/BCT model of dendrite growth [4, 5]. As it has been shown in [1,2], the increase of undercooling leads to solute trapping with the deviation from local chemical equilibrium at the solid-liquid interface in rapid solidification. In the LKT/BCT model of dendrite growth [4, 5], this phenomenon is introduced by the solute partitioning function $k(V)$ which adopts interfacial diffusion speed V_{DI} as a kinetic parameter of rapid solidification [6]. Experimentally, the diffusion speed V_{DI} has been independently determined by pulsed laser experiments [1] on thin specimens for the $Ni_{99}Zr_1$ alloy. Together with preliminary used parameters of Ni-Zr alloys, the measured results for V_{DI} encouraged the prospects of a parameter-free test of the LKT/BCT model. In addition, the dendritic structure of solidified droplets from $Ni_{99.5}Zr_{0.5}$ and $Ni_{99}Zr_1$ alloys has been evaluated [2] to find morphological transitions in dendritic pattern. The results of metallographic analysis were compared with the predictions of Karmas model [7, 8] on grain refinement *via* dendritic fragmentation.

Selected and novel results of computational experiments on rapid dendritic growth in Ni and Ni-Zr alloys are summarized in the present paper. Predictions of a model for rapid dendritic growth, which assumes deviation from local equilibrium at the interface and in the solute

diffusion field, are presented. An influence of the small quantity of Zr on growth of nickel dendrites are shown.

2. Governing equations

The mathematical model for the dendrite growth is described and tested in a growth of TiAl crystals in [9]. Particularly, the growth of a parabolic needle-like dendrite with the four-fold symmetry of anisotropic properties has been analyzed with taking into account of local non-equilibrium conditions in the solute diffusion field and at the solid-liquid iterface. Neglecting the diffusion in the solid phase, the concentration field in the liquid is governed by the following mass transport equation

$$\tau_D \frac{\partial^2 C_l}{\partial t^2} + \frac{\partial C_l}{\partial t} + (\vec{w} \cdot \vec{\nabla}) C_l = D_C \nabla^2 C_l, \tag{1}$$

where C_l is the solute concentration in the liquid, $\vec{w}$ is the flow velocity, D_C is the diffusion coefficient of the solute, t is the time and τ_D is the relaxation time of the diffusion flux to its steady state.

Experimental measurements of fast dendritic growth cover the range of crystal growth velocities which can be smaller, comparable or even greater than the characteristic solute diffusion speed in bulk phases but they are still much smaller than the characteristic speed of heat propagation [10]. Therefore, while the mass transport can be described by the hyperbolic equation 1 which includes the finite value of the diffusion speed $V_D = (D_C/\tau_D)^{1/2}$, the evolution of the temperature field is described by a parabolic equation which assumes an infinite speed for the heat propagation. Designating T_l and T_s as temperatures in the liquid and solid phases, one can write

$$\frac{\partial T_l}{\partial t} + (\vec{w} \cdot \vec{\nabla}) C_l = D_T \nabla^2 T_l, \quad \frac{\partial T_s}{\partial t} = D_T \nabla^2 T_s, \tag{2}$$

where D_T stands for the thermal diffusivity.

At the dendritic interface, conservation of mass and energy yields boundary conditions of the form

$$\tau_D \frac{\partial}{\partial t} \left[(C_l - C_s) \vec{v} \cdot \vec{n} \right] + (C_l - C_s) \vec{v} \cdot \vec{n} + D_C \vec{\nabla} C_l \cdot \vec{n} = 0, \tag{3}$$

$$T_Q \vec{v} \cdot \vec{n} = D_T \left(\vec{\nabla} T_s - \vec{\nabla} T_l \right) \cdot \vec{n}, \tag{4}$$

where $\vec{n}$ is the unit vector normal to the dendrite interface, $\vec{v}$ is the interface velocity, $C_s = k_v C_l$ is the concentration in the solid phase at the dendritic interface, k_v is the velocity dependent solute distribution coefficient, $T_Q = Q/c_p$, Q is the latent heat released per unit volume of solidified matter and c_p is the heat capacity.

The temperature at the dendrite interface $T_i = T_l = T_s$ is connected to the crystallization temperature T_0 of the pure liquid, the local curvature $2/R$ of the front, the liquid concentration C_l, and the intensity of atomic flux providing the normal growth velocity $(\vec{v} \cdot \vec{n}) = v_n$ by

$$T_i = T_0 - m_v C_l - Q c_p^{-1} 2 R^{-1} d(\theta) - \tilde{\beta}(\theta) v_n. \tag{5}$$

Here θ is the angle between the normal to the dendrite interface and its preferred growth direction (e.g., $< 001 >$ directions for fcc crystals), $\tilde{\beta}$ is the anisotropic coefficient of growth, $d(\theta)$ is the anisotropic capillary length, and m_v is the velocity-dependent liquidus line slope in the kinetic phase diagram of a binary system.

Anisotropic properties of the interface, such as surface energy, depend on the spherical angles which define the orientation of the normal to the dendrite interface to its growth direction. Considering a case of axisymmetric needle-like crystal one can apply averaging over one spherical

angle and essentially simplify analytical form of the anisotropic properties of the crystal-liquid interface [11]. As a result of such averaging for the cubic crystal symmetry, the capillary length $d(\theta)$ and kinetic coefficient $\beta(\theta)$ are represented as

$$d(\theta) = d_0 \left\{1 - \alpha_d \cos\left[4\left(\theta - \theta_d\right)\right]\right\}, \tag{6}$$

$$\tilde{\beta}(\theta) = \beta_0 Q c_p^{-1} \left\{1 - \alpha_\beta \cos\left[4\left(\theta - \theta_\beta\right)\right]\right\}, \tag{7}$$

where d_0 and β_0 are the capillary and kinetic constants, $\alpha_d \ll 1$ and $\alpha_\beta \ll 1$ are the anisotropy parameters whereas θ_d and θ_β represent the angles between the direction of growth and the preferred growth directions, which correspond to the minima of $d(\theta)$ and $\beta(\theta)$.

Far from the dendritic surface the solute concentration, the temperature and the flow velocity in the liquid are fixed, i.e.

$$C_l = C_\infty, \quad T_l = T_\infty, \quad |\vec{w}| = U, \tag{8}$$

U being the characteristic flow velocity far from the dendrite. A family of exact solutions of the hydrodynamic problem can be found in two cases when the fluid flow is potential or of Oseen type. Here, the more realistic case of viscous flow described by the so-called Oseen and mass conservation equations is considered:

$$U\frac{\partial \vec{w}}{\partial z} = -\frac{1}{\rho_1}\vec{\nabla} p + \nu \nabla^2 \vec{w}, \quad \vec{\nabla} \cdot \vec{w} = 0, \tag{9}$$

where z is the direction of dendritic growth, ρ_1 is the liquid density and ν is the kinematic viscosity. Equations 6 should be solved with no-slip boundary conditions for the fluid velocity.

The system of equations (1)-(6) couples the concentration and the thermal problem and describes the growth of a parabolic dendrite under local non-equilibrium conditions in the diffusion field and at the solid-liquid interface. It extends the previous problem considered by Ben Amar and Pelcé [12] for anisotropic dendrite growth under local equilibrium conditions, generalizes the study of Ref. [13] for sufficiently large growth rates in the local equilibrium limit, and, finally, advances the isotropic description [14, 15] of the local non-equilibrium dendrite growth.

In the modeling we consider the steady state tip of a needle-like dendrite with radius R propagating with constant velocity $V = v_n$. The selection criterion for the steady state dendritic growth can be found by the combination of previously obtained solutions, which describe the anisotropic dendrite growing in the presence of convective flow [16] and the local non-equilibrium dendritic growth in rapid solidification processes without convection [17]. On the basis of these advancements, a sharp interface model for steady-state dendrite has been formulated [9] which is used in the present work to evaluate growth kinetics of a pure nickel dendrites with a small amount of zircon.

3. Results and discussion

The sharp interface model [9] based on equations (1)-(6) has been used without convective flow, i.e. at $U = 0$. To study the influence of a change of growth velocity by small amounts of strongly partitioning impurities a pure Ni-dendrites with small amounts of zircon (0.1 at.%Zr, 0.5 at.%Zr and 1 at.%Zr) have been taken for the calculations. For evaluation of the dendrite growth kinetics the relationship “dendrite tip radius - undercooling” and “dendrite growth velocity - undercooling” have been computed using the materials parameters from Table 1. The results of computations are shown in Figs. 1 and 2.

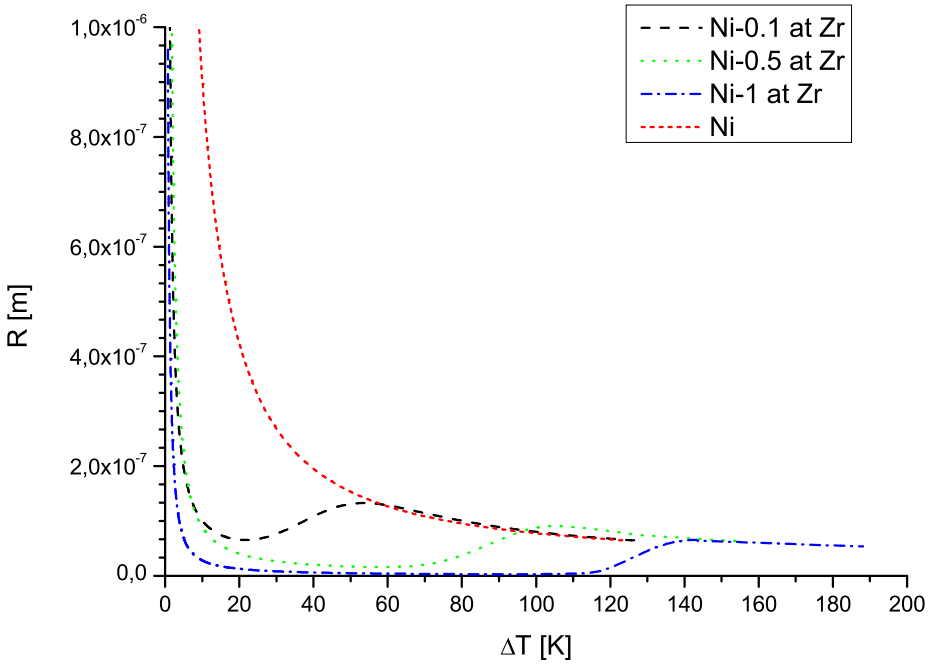

Figure 1. Computed dendrite tip radius for pure Ni, and different dilute Ni-based alloys $Ni_{99.9}Zr_{0.1}$, $Ni_{99.5}Zr_{0.5}$ and $Ni_{99}Zr_1$.

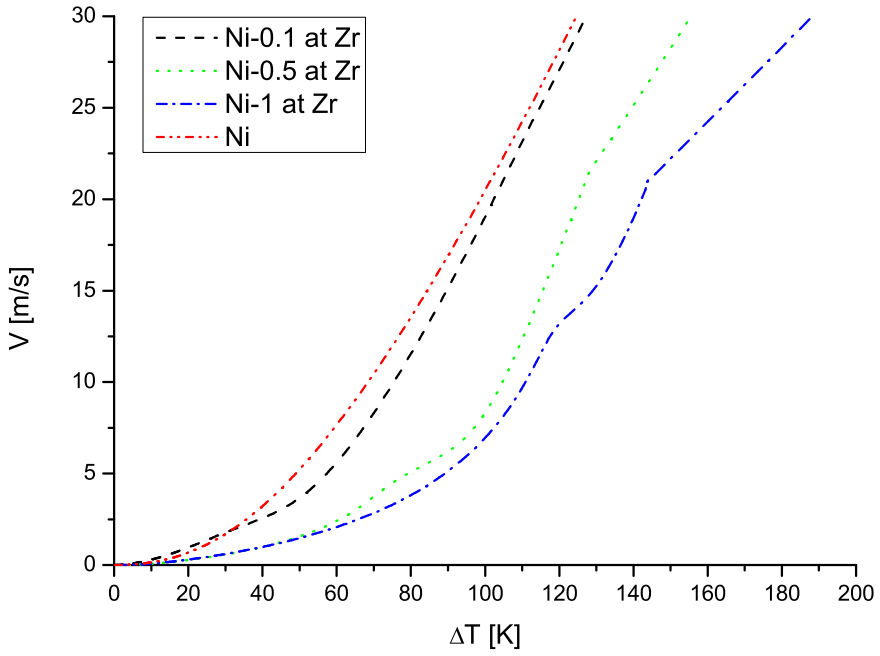

Figure 2. Comparison of dendrite growth velocities as a function of undercooling for pure Ni, and different dilute Ni-based alloys: $Ni_{99.9}Zr_{0.1}$, $Ni_{99.5}Zr_{0.5}$ and $Ni_{99}Zr_1$, as calculated within the sharp interface model [9].

Table 1. Material parameters for Ni and NiZr used in calculations as is given in Refs. [18, 19].

Material parameter	Dimension	Pure Ni	Ni–0.1 at.%Zr	Ni–0.5 at.%Zr	Ni–1 at.%Zr
Nominal concentration, C_∞	at.%	0	0.1	0.5	1
Melting temperature, T_m	K	1728	1728	1728	1728
Thermal diffusivity, D_T	m^2/s	$1.2 \cdot 10^{-5}$	$1.2 \cdot 10^{-5}$	$1.2 \cdot 10^{-5}$	$4.2 \cdot 10^{-5}$
Diffusion coefficient, D_C	m^2/s	–	$2.5 \cdot 10^{-9}$	$2.5 \cdot 10^{-9}$	$2.5 \cdot 10^{-9}$
Equilibrium partition coefficient, k_e		–	0.02	0.03	0.04
Liquidus slope, m_e	K/at.%	–	-9	-10	-11
Capillary constant, d_0	m	$7.89 \cdot 10^{-10}$	$7.89 \cdot 10^{-10}$	$7.89 \cdot 10^{-10}$	$2.02 \cdot 10^{-10}$
Kinetic growth coefficient, μ_k	$m/s/K$	0.59	0.59	0.42	0.22
Strength of the surface energy anisotropy, α_d		0.66	0.66	0.675	0.75
Bulk diffusion speed, V_D	m/s	–	23.5	21.5	21
Interface diffusion speed, V_{DI}	m/s	–	22.5	20	20.5
Latent heat of crystallization, Q	J/mol	17150	17150	16700	16230
Heat capacity, c_p	J/mol/K	41	41	41	41

The relation "tip radius – undercooling" clearly demonstrates the influence of doping a pure metal with very small amounts . Figure 1 shows the dendrite tip radius of pure Ni and various dilute Ni-based alloys as a function of undercooling. While in the case of pure Ni the tip radius is purely thermally controlled and decreases monotonically with the increase of undercooling, the addition only of 0.1 at.%Zr (as a strongly partitioning element in Ni-based alloys) leads to an essential change in the dendrite tip radius. The tip radius decreases essentially in comparison with the thermally controlled growth of dendrite tip of the pure Ni. Dendrite growth in the Ni-0.1 at.%Zr alloy melt becomes purely solute diffusion limited with the characteristic lengths much smaller than the thermal length which is dictated the tip radius of a pure nickel dendrite. This is typical example of the growth of the so-called "chemical dendrite" (which is also entitled as "solutal dendrite"). As it can be seen in example of the Ni-0.1 at.%Zr alloy's dendrite, the gradual decreasing of the tip radius occurs up to approximately $\Delta T = 22$K (see Fig. 1). As the sharp interface model [9] predicts, around this undercooling, the characteristic length for diffusion Zr atoms becomes comparable with the capillary length of the solid-liquid interface and the transition from the curved paraboloidal dendrite to the planar interface begins. Therefore, the dendrite tip radius growing in the Ni-0.1 at.%Zr alloy begins to increase at $\Delta T > 22$K. However, transformation of the chemical dendrite to the planar interface can not be proceed to its end due to solidification of the non-isothermal melt that exhibit thermal lengths scale to define a growth of the thermal dendrite. The Ni-0.1 at.%Zr alloy's dendrite reaches thermal length scale approximately at $\Delta T = 60$K (see Fig. 1). In this particular case, the transition from chemical dendrite to thermal dendrite occurs in the range of undercooling $22 \leq \Delta T\text{K} \leq 60$ and the tip radius of the Ni-0.1 at.%Zr alloy's dendrite almost confluence with the behavior of the tip radius of the pure nickel dendrite at $\Delta T\text{K} > 60$ (see Fig. 1). The transition is completely finished at the dendrite tip velocity V equals the diffusion speed V_D in the bulk melt, $V = V_D$ [14, 15]. For the Ni-0.1 at.%Zr alloy's dendrite, this occurs with the undercooling $\Delta T[V = V_D = 23.5(\text{m/s})] = 110$K (see Table 1 and Fig. 1). With $\Delta T \geq \Delta T[V = V_D]$, the solidification proceeds by the diffusionless mechanism and the main stem of the alloy's dendrite growth as the dendritic stem in a pure melt. The diffusionless mechanism of solidification means chemically partitionless solidification without solute redistribution ahead and at the solid-liquid interface. Such mechanism is the result of the complete solute trapping by the dendritic tips. In this case, solid phase forms with the initial (nominal) chemical compositions. Because we consider steady state growth of the dendrite tip, the dendrite stem behind the tip forms without chemical inhomogeneity at $C_s(V \geq V_D) = C_\infty$.

The same tendency have other diluted alloys, Ni-0.5 at.%Zr and Ni-1 at.%Zr (see Fig. 1). However, the minimum and maximum in the function $R(\Delta T)$ of these alloying dendrites are shifted to the larger undercooling as the concentration of Zr increases. This indicates more pronounced constitutional effect with the increase of Zr in the diluted nickel based alloys (for the present case, in the diluted nickel based alloys).

Table 2. Material parameters for Ni and NiZr used in calculations as is given in Refs. [18, 19].

Material parameter	Dimension	Pure Ni	Ni–0.01 at.%Zr	Ni–0.1 at.%Zr
Nominal concentration, C_∞	at.%	0	0.01	0.1
Melting temperature, T_m	K	1728	1728	1728
Thermal diffusivity, D_T	m^2/s	$1.2 \cdot 10^{-5}$	$1.2 \cdot 10^{-5}$	$1.2 \cdot 10^{-5}$
Diffusion coefficient, D_C	m^2/s	–	$2.5 \cdot 10^{-9}$	$2.5 \cdot 10^{-9}$
Equilibrium partition coefficient, k_e		–	0.02	0.02
Liquidus slope, m_e	K/at.%	–	-9	-9
Capillary constant, d_0	m	$7.89 \cdot 10^{-10}$	$7.89 \cdot 10^{-10}$	$7.89 \cdot 10^{-10}$
Kinetic growth coefficient, μ_k	$m/s/K$	0.59	0.59	0.59
Strength of the surface energy anisotropy, α_d		0.66	0.66	0.66
Bulk diffusion speed, V_D	m/s	–	23.5	23.5
Interface diffusion speed, V_{DI}	m/s	–	22.5	22.5
Latent heat of crystallization, Q	J/mol	17150	17150	17150
Heat capacity, c_p	J/mol/K	41	41	41

Figure 2 shows the results of the growth velocity as a function of undercooling in the pure Ni-melt and in the dilute Ni-Zr alloy melts. In the very dilute alloy $Ni_{99.9}Zr_{0.1}$ an enhancement of the velocity is observed compared with the velocity of pure Ni that occurs for the uncerooling $\Delta T < 35$K. The other alloys with higher concentrations show a decrease of the velocity with the undercooling in comparison with the velocity of the pure nickel dendrite. Furthermore the decrease in velocity of the $Ni_{99}Zr_1$-dendrite being more pronounced than the velocity of the $Ni_{99.5}Zr_{0.5}$-dendrite. Apparently, there are two counteracting effects of the addition of impurities, one leading to an increase of the growth dynamics in particular at the very dilute limit and the other one decreasing the growth velocity the latter one dominating at higher concentrations. Indeed, since the chemical diffusion coefficient is about three to four orders of magnitude smaller than the thermal diffusivity the chemical dendrites become narrow because of the strong concentration gradient and they are broaden when reaching the limit of absolute chemical stability. This effect is responsible for the enhancement of the dendrite growth velocity of very dilute alloys at small undercooling since a thin dendrite propagates faster than a thick dendrite. In addition to this, constitutional effect in the stability of a growing dendrite the solute causes a constitutional undercooling that requires solute redistribution and therefore, makes the dendrite growth more sluggish. The effect of velocity enhancement dominates at small concentration whereas the effect of constitutional undercooling predominates at larger concentrations.

To confirm the enhancement of velocity due to the tiny amount of impurity in comparison with the velocity of the pure dendrite, we specially computed growth velocity for dendrites growing from undercooled pure Ni, binary $Ni_{99.99}Zr_{0.01}$ and $Ni_{99.9}Zr_{0.1}$ alloys. The material parameters for pure Ni, binary $Ni_{99.99}Zr_{0.01}$ and $Ni_{99.9}Zr_{0.1}$ alloys are presented in the Rable 2. Figure 3 shows behavior of the tip velocity as the logarithmic function of small undercoolings. The velocity of the $Ni_{99.99}Zr_{0.01}$-dendrite also larger then the velocity of the pure Ni-dendrite in the range $\Delta T < 35$K. This, indeed, confirms the fastest growth of the narrow chemical dendrites at small quantity of impurity in comparison with the thicker thermal dendrites. However, Fig.

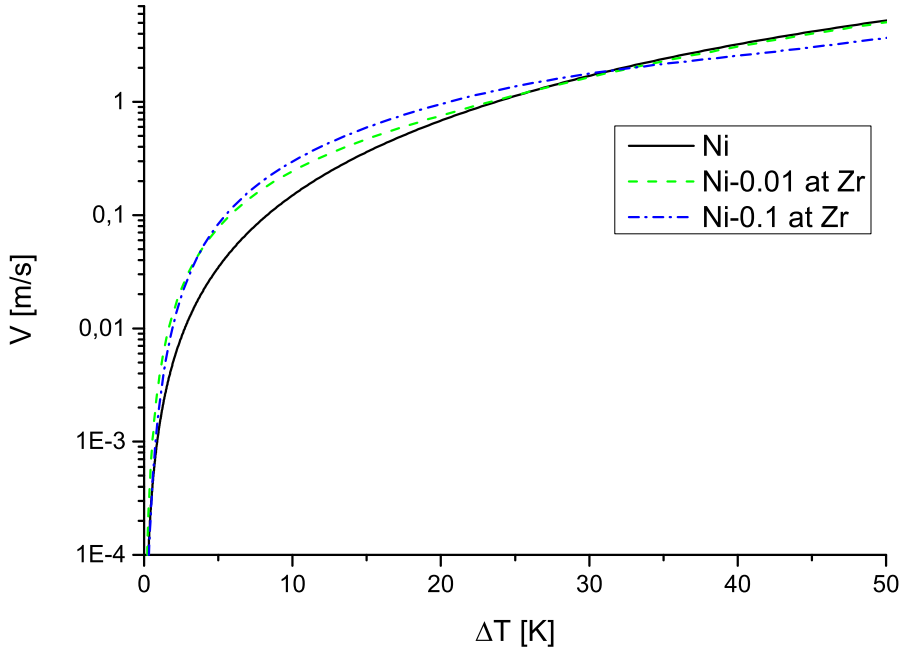

Figure 3. Effect of dendrite growth velocity enhancement in very diluted alloys. It is shown that the tips of alloying dendrites, $Ni_{99.99}Zr_{0.01}$ and $Ni_{99.9}Zr_{0.1}$, are growing faster than the tip of the pure nickel dendrite in the range of undercooling $\Delta T < 35$K.

3 also demonstrates that the $Ni_{99.99}Zr_{0.01}$-dendrite grows slower than the $Ni_{99.9}Zr_{0.1}$-dendrite. As a results of such non-linear dependence at $\Delta T < 35$K, we have obtained the following sequence of the growth velocities:

$$V_{Ni_{99.5}Zr_{0.5}} < V_{Ni} < V_{Ni_{99.99}Zr_{0.01}} < V_{Ni_{99.9}Zr_{0.1}}.$$

This means, between concentrations 0.1%Zr and 0.5%Zr, there is a Ni-Zr content which leads to the biggest enhancement of the dendrite velocity (in comparison with the velocity of the pure Ni-dendrite). This effect of non-linear influence of the impurity on the growth velocity can be considered in our future work.

4. Conclusions

Computational results on primary dendrite solidification have been obtained using the sharp interface model [9]. The kinetics has been eveluated by the dendrite tip radius and growth velocity of dendrites growing in undercooled melts of nickel and dilute Ni-Zr alloys. A transition from chemical dendrite to the thermal dendrite has been demonstrated in a whole range of undercooling. It has been demonstrated that small amounts of Zr lead to the increase of the growth velocity in the range of small undercoolings. This effect of the dendrite velocity enhancement by tiny amonts of impurity should be investigated more detailed due to its non-linearity: there is a critical concentration of Zr at which one may find the biggest enhancement of the dendrite velocity (in comparison with the velocity of the pure dendrite). These outcomes might be investigated experimentally and computationally using a phase field computational technique.

5. References

[1] Arnold C B, Aziz M, Schwarz M, Herlach D M 1999 *Phys. Rev. B* **59** 334-343
[2] Schwarz M 1998 Kornfeinung durch Fragmentierung von Dendriten *Ph.D. Thesis (Ruhr-Universitt Bochum*
[3] Herlach D M, Annu. 1991 *Rev. Mater. Sci.* **21** 23-44
[4] Lipton J, Kurz W, Trivedi R 1987 *Acta Metall.* **35** 957-964
[5] Boettinger W J, Coriell S R, Trivedi R 1988 Rapid Solidification Processing: Principles and Technologies IV *Editors: R. Mehrabian and P. Parrish (Claitors, Baton Rouge, Louisiana* 13
[6] Aziz M, Kaplan T 1988 *Acta Metall.* **36** 2335-2347
[7] Schwarz M, Karma A, Eckler K, Herlach D M 1994 *Phys. Rev. Lett.* **73** 1380-1383
[8] Karma A 1998 Int. J. Non-Equilibrium Processing **11** 201-233
[9] Galenko P K, Danilov D A, Reuther K, Alexandrov D V, Rettenmayr M, Herlach D M 2017 Effect of convective flow on stable dendritic growth in rapid solidification of a binary alloy *Journal of Crystal Growth* **457** 349355
[10] Herlach D, Galenko P, and Holland-Moritz D 2007 Metastable Solids from Undercooled Melts *Elsevier, Amsterdam*
[11] Barbieri A, and Langer J S 1989 Predictions of dendritic growth rates in the linearized solvability theory *Phys. Rev. A* **39** 5314-5325
[12] Ben Amar M, Pelcé P 1989 Impurity effect on dendritic growth *Phys. Rev. A* **39** 4263-4269
[13] Alexandrov D V, Galenko P K 2013 Selection criterion of stable dendritic growth at arbitrary Peclétnumbers with convection *Phys. Rev. E* **87** 062403
[14] Galenko P K, Danilov D A 1997 Local nonequilibrium effect on rapid dendritic growth in a binary alloy melt *Physics Letters A* **235** 271-280
[15] Galenko P K, Danilov D A 1999 Model for free dendritic alloy growth under interfacial and bulk phase nonequilibrium conditions *Journal of Crystal Growth* **197** 992-1002
[16] Alexandrov D V, Galenko P K 2015 Thermo-solutal and kinetic regimes of an anisotropic dendrite growing under forced convective flow *Phys. Chem. Chem. Phys.* **17** 19149-19161
[17] Alexandrov D V, Danilov D A, and Galenko P K 2016 Selection criterion of a stable dendrite growth in rapid solidification *Int. J. Heat Mass Transfer* **101** 789799
[18] Galenko P K, Phanikumar G, Funke O, Chernova L, Reutzel S, Kolbe M, Herlach D M 2007 Dendritic solidification and fragmentation in undercooled NiZr alloys *Materials Science and Engineering A* **449451** 649653
[19] Herlach D M, Galenko P K 25 March 2007 Rapid solidification: in situ diagnostics and theoretical modelling *Materials Science and Engineering: A* **449-451** 34-41

Acknowledgments

O. V. K. acknowledges support of RFBR by the project No. 16-38-60172 mol_a_dk and a program "Postdocs of UrFU". P. K. G. and D. V. A. acknowledge support from the RSF, grant number 16-11-10095. P. K. G. also acknowledges support under the project "MULTIPHAS", contract Nr. 50WM1541 by the European Space Agency, German Aerospace Center and Friedrich-Schiller-Universität Jena.